Progress In Electromagnetics Research, Vol. 131, 169–184, 2012

TRANSMISSION THROUGH TWISTED CLAD LIQUID CRYSTAL OPTICAL FIBERS

P. K. Choudhury*

Institute of Microengineering and Nanoelectronics (IMEN), Universiti Kebangsaan Malaysia, UKM, Bangi, Selangor 43600, Malaysia

Abstract—The paper presents an analytical investigation of three-layer twisted clad liquid crystal fiber in respect of its power propagation characteristics. The fiber under consideration has dielectric non-magnetic materials in its core and inner clad sections, whereas the outermost clad is made of radially anisotropic liquid crystal material. Twist in the fiber is introduced in the form of superfine helical turns at the interface of the core and the inner clad regions with specified values of pitch angle. Results demonstrate large confinement of optical power in the outermost liquid crystal section. Further, the angle of twist is seen to have its pronounced effect on controlling the flow of power as it exhibits the ability of governing the propagation characteristics of the medium. The observed propagation feature is attributed to the radial anisotropy of the liquid crystal outer region as well as the amount of twist introduced, and attracts useful applications of such complex fiber structures in evanescent field optical sensing and other coupling devices primarily used in integrated optics.

1. INTRODUCTION

Several research reports have appeared in the literature on the development of different types of materials and composites to tailor or manipulate the propagation characteristics of optical waveguides owing to its greatly depending on the materials in use. In that stream, various forms of complex structures have also been investigated. Indeed, the use of materials as well as structures remains extremely purpose oriented. Among the others, optical fibers made of liquid crystals have been attractive for multifarious applications, particularly in the area of integrated optics, because of their possessing distinct anisotropic

Received 13 June 2012, Accepted 24 August 2012, Scheduled 6 September 2012

* Corresponding author: Pankaj Kumar Choudhury (pankaj@ukm.my).

characteristics in their physical properties [1–5]. Furthermore, the macroscopic optical properties of liquid crystals can be greatly altered under the influence of external electric field [6]. In reality, liquid crystals exhibit the largest electro-optic effect among known materials, which makes them much demanding for various technological needs.

Investigators have studied liquid crystal optical fibers (LCFs) of different kinds of constructions in respect of geometry as well as material distribution [7, 8]. High anisotropic property of liquid crystals makes LCFs to be characterized by polarization anisotropy. The efficacy of the use of LCFs has been in the fabrication of directional couplers, optical switches, modulators, sensors etc. [9–14]. In most of the applications, conventional optical fibers are cladded with liquid crystals. However, studies have also been reported for LCFs with liquid crystal core [4, 5].

Fibers with helical structures, which fall into the category of complex mediums, have also attracted investigators primarily because the angle of pitch of the helix in use exhibits dominant characteristics to alter the wave propagation characteristics of the guide. This is based on the conceptual understanding of low- and medium-power traveling wave tubes (TWTs) [15], the analysis of which generally includes waveguides under slow-wave structures with conducting sheath and tape helixes. Implementing the concept in the case of optical fibers, studies have been reported corresponding to dielectric circular and elliptical fibers [16–22].

Motivation of the present paper comes from the idea of amalgamating the properties of liquid crystals as well as helical structures into the guide. The investigation is aimed at the propagation characteristics of the three-layer fiber structure with liquid crystal clad having twists imposed in the form of conducting helical wraps on the core-inner clad boundary emphasizing the transmission of power through it; the core and the inner clad section are assumed to be homogeneous dielectrics. The implementation of helical windings makes the analysis much rigorous. However, such purposely introduced wraps develop the property to control the dispersion characteristics of the guide.

In the present communication, we consider the case of sheath helix [22] which has vanishing conductivity in a direction normal to the direction of conduction. Furthermore, the liquid crystal section of the guide is assumed to have radial orientation of molecules (i.e., the outermost section of the guide attains a radial anisotropy), which may be evolved by capillary action after inserting the liquid crystal section (of the fiber) into a capillary tube coated with N, N-dimethyl-N-octadecyl-3-aminopropyltrimethoxysilyl chloride [8]. Since the

propagation of power through a guide is greatly important to assess the possible applications, the relative distribution of power has been studied for the different sections of the guide under consideration corresponding to the different values of pitch angle (e.g., 0°, 45° and 90°), and it has been found that the confinement of power remains maximum in the outermost liquid crystal section. Further, the propagation of power can be controlled by varying the angle of pitch of the introduced helical wraps. This gives the illuminating idea of applications of such type of guides for possible sensing needs where the controls over the waveguide remain vital during the operation.

2. THEORY

Figure 1(a) shows the longitudinal view of the helical clad liquid crystal fiber (HCLCF), which is essentially a three-layer cylindrical waveguide with the outermost cladding filled with liquid crystal material, and the fiber core is wrapped with a conducting sheath helix. We consider the infinitely extended radially asymmetric liquid crystal clad, which imposes the liquid crystal molecules to have radial orientation (the cross-sectional view of the guide is depicted in Figure 1(b) where the dashed lines indicate the orientation of liquid crystal molecules in the radial direction). Thus, the structure essentially has a circular cylindrical surface with high conductivity in a preferential direction, and having helical windings at a constant angle (called as the helix pitch angle) ψ around the core-inner clad boundary. It is noteworthy

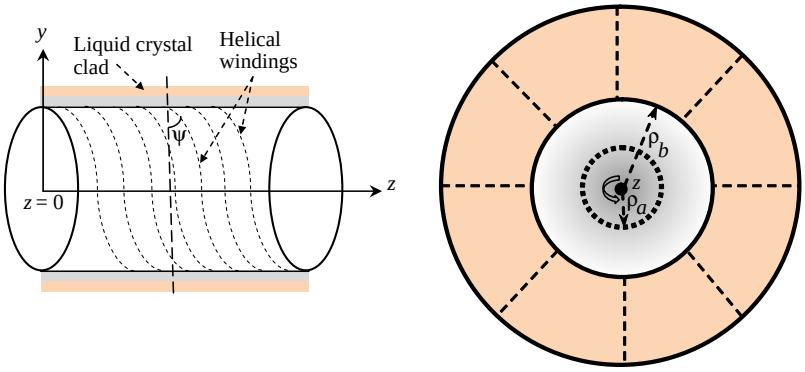

Figure 1. (a) Longitudinal view of the HCLCF under consideration. (b) Cross-sectional view of a three-layer HCLCF with the outermost section filled with liquid crystal (the dashed lines in the radial direction indicate the orientation of liquid crystal molecules).

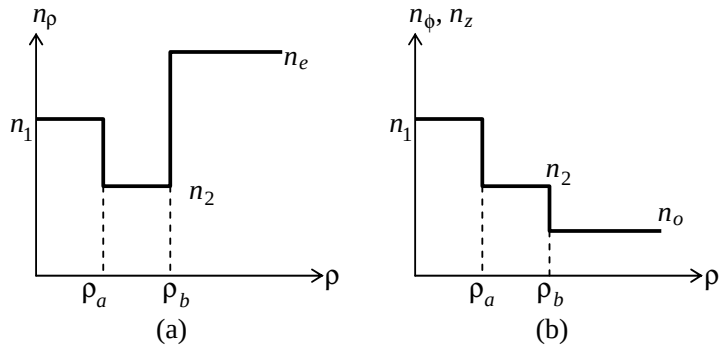

Figure 2. The RI distribution pattern.

that the pitch angle can be effectively used to control the modal behaviour of the HCLCF under consideration, and serves as an additional controlling parameter, which may find great technological importance [19–22]. We assume that the core and the inner clad regions of the HCLCF are homogeneous, isotropic and non-magnetic with the refractive index (RI) values as n_1 and n_2 (with $n_1 > n_2$), respectively, along with their respective radii values as ρ_a and ρ_b. Furthermore, the liquid crystal section has the respective ordinary and the extraordinary RI values as n_o and n_e. We consider the principal axes of the outer clad to coincide with the optical axis along the z-direction, and the extraordinary principal axis attains a radial orientation. As such, the outermost liquid crystal clad will have the RI distributions as $n_\rho = n_e$ and $n_\phi = n_z$ with $n_e > n_1 > n_2 > n_o$, as illustrated in Figure 2. The anisotropic nature of the HCLCF will make the modes to contain the three electric field components E_ρ, E_ϕ and E_z to face different RI values in their respective directions.

Now, considering the time t- and the axis z-harmonic electromagnetic fields to propagate through the HCLCF, the coupled equations for the transverse field components can be written as [23, 24]

$$\left(\nabla_t^2 + k_0^2 n_\rho^2 - \beta^2 - \frac{1}{\rho^2}\right) e_\rho = -\frac{2}{\rho^2}\frac{\partial e_\phi}{\partial \phi} + \left(1 - \frac{n_\rho^2}{n_z^2}\right)\frac{\partial}{\partial \rho}\left\{\frac{1}{\rho}\frac{\partial}{\partial \rho}(\rho e_\rho)\right\} + \left(1 - \frac{n_\phi^2}{n_z^2}\right)\frac{\partial}{\partial \rho}\left(\frac{1}{\rho}\frac{\partial e_\phi}{\partial \phi}\right) \quad \text{(1a)}$$

and

$$\left(\nabla_t^2 + k_0^2 n_\phi^2 - \beta^2 - \frac{1}{\rho^2}\right) e_\phi = \frac{2}{\rho^2}\frac{\partial e_\rho}{\partial \phi} + \frac{1}{\rho^2}\left\{\left(1 - \frac{n_\rho^2}{n_z^2}\right)\frac{\partial}{\partial \rho}\left(\rho \frac{\partial e_\rho}{\partial \phi}\right) + \left(1 - \frac{n_\phi^2}{n_z^2}\right)\frac{\partial^2 e_\phi}{\partial \phi^2}\right\} \quad \text{(1b)}$$

with ∇_t^2 as the Laplacian operator in the cylindrical coordinate system; n_ρ, n_ϕ and n_z as the RI values along the ρ-, ϕ- and z-directions, respectively, and k_0 as the free-space propagation constant. Following some tedious mathematical steps, it can be shown that, in the case of transverse electric modes, the field components in the three different regions of the HCLCF can be expressed as

$$H_{\rho_1} = -C_{\phi_1} \frac{\beta}{\omega\mu_0} J_1(\gamma_1\rho) \exp\{i(\omega t - \beta z)\} \quad \text{for } \rho \le \rho_a \tag{2a}$$

$$H_{z_1} = C_{\phi_1} \frac{i}{\omega\mu_0} \left\{\gamma_1 J_1'(\gamma_1\rho) + \frac{1}{\rho} J_1(\gamma_1\rho)\right\} \exp\{i(\omega t - \beta z)\} \quad \text{for } \rho \le \rho_a \tag{2b}$$

$$H_{\rho_2} = -\frac{\beta}{\omega\mu_0} \{C_{\phi_2} K_1(\gamma_2\rho) + C_{\phi_3} I_1(\gamma_2\rho)\} \exp\{i(\omega t - \beta z)\} \quad \text{for } \rho_b \ge \rho \ge \rho_a \tag{3a}$$

$$H_{z_2} = \frac{i}{\omega\mu_0} \left[C_{\phi_2} \left\{\gamma_2 K_1'(\gamma_2\rho) + \frac{1}{\rho} K_1(\gamma_2\rho)\right\} + C_{\phi_3} \left\{\gamma_2 I_1'(\gamma_2\rho) + \frac{1}{\rho} I_1(\gamma_2\rho)\right\} \exp\{i(\omega t - \beta z)\} \quad \text{for } \rho_b \ge \rho \ge \rho_a \right. \tag{3b}$$

$$H_{\rho_3} = -C_{\phi_4} \frac{\beta}{\omega\mu_0} K_1(\gamma_3\rho) \exp\{i(\omega t - \beta z)\} \quad \text{for } \rho \ge \rho_b \tag{4a}$$

$$\text{and } H_{z_3} = C_{\phi_4} \frac{i}{\omega\mu_0} \left\{\gamma_3 K_1'(\gamma_3\rho) + \frac{1}{\rho} K_1(\gamma_3\rho)\right\} \exp\{i(\omega t - \beta z)\} \quad \text{for } \rho \ge \rho_b \tag{4b}$$

In these equations, ω is the angular frequency of the wave in the unbounded medium, β the propagation constant in the axial direction, μ_0 permeability of the free-space, and C_{ϕ_1}, C_{ϕ_2}, C_{ϕ_3} and C_{ϕ_4} are the arbitrary constants to be determined by implementing the boundary conditions. Also, the quantities γ_1, γ_2 and γ_3 are defined as follows:

$$\gamma_1 = \sqrt{n_1^2 k_0^2 - \beta^2} \tag{5a}$$

$$\gamma_2 = \sqrt{\beta^2 - n_2^2 k_0^2} \tag{5b}$$

$$\text{and} \quad \gamma_3 = \sqrt{\beta^2 - n_o^2 k_0^2} \tag{5c}$$

It is noteworthy that the conductivity of the sheath helix in use is zero in a direction normal to the conduction. Considering the tangential field components in the direction of conductivity, the continuity conditions [25] for the guiding structure under consideration state that the tangential components of the electric and the magnetic fields must satisfy the following equations at the boundary:

$$E_{z_1} \sin\psi + E_{\phi_1} \cos\psi = 0 \tag{6a}$$

$$E_{z_2}\sin\psi + E_{\phi_2}\cos\psi = 0 \tag{6b}$$

$$(E_{z_1} - E_{z_2})\cos\psi - (E_{\phi_1} - E_{\phi_2})\sin\psi = 0 \tag{7a}$$
$$(H_{z_1} - H_{z_2})\sin\psi + (H_{\phi_1} - H_{\phi_2})\cos\psi = 0 \tag{7b}$$

$$E_{z_2}\sin\psi + E_{\phi_2}\cos\psi = 0 \tag{8a}$$
$$E_{z_3}\sin\psi + E_{\phi_3}\cos\psi = 0 \tag{8b}$$

$$(E_{z_2} - E_{z_3})\cos\psi - (E_{\phi_2} - E_{\phi_3})\sin\psi = 0 \tag{9a}$$
$$\text{and} \quad (H_{z_2} - H_{z_3})\sin\psi + (H_{\phi_2} - H_{\phi_3})\cos\psi = 0 \tag{9b}$$

In these equations, the suffices 1, 2 and 3, respectively, represent the situations in the core, the inner clad and the outermost liquid crystal regions. Using these field components, as stated in Eqs. (2), (3) and (4), and implementing the conditions of continuity in Eqs. (6)–(9), the values of the arbitrary constants C_{ϕ_1}, C_{ϕ_2}, C_{ϕ_3} and C_{ϕ_4} can be determined. Finally, after some tedious mathematical steps, the power [26] transmitted through the different sections of the HCLCF can be deduced as

$$P_c = \pi \left| \mathrm{Re} \left[\int_0^{\rho_a} J_\nu(\gamma_1\rho) \times \frac{i}{\gamma_1^2} \left\{ \frac{i\nu\beta}{\rho} \Omega J_\nu(\gamma_1\rho) + \omega\varepsilon_1\gamma_1 J'_\nu(\gamma_1\rho) \right\} \right.\right.$$
$$\left.\left. -\Omega J_\nu(\gamma_1\rho) \frac{i}{\gamma_1^2} \left\{ \frac{i\nu\beta}{\rho} J_\nu(\gamma_1\rho) - \omega\mu_0\Omega\gamma_1 J'_\nu(\gamma_1\rho) \right\} \right] \rho d\rho d\phi \right| \tag{10}$$

$$P_{ic} = \pi \left| \int_{\rho_a}^{\rho_b} \mathrm{Re} \left[\{\Theta K_\nu(\gamma_2\rho) + \Lambda I_\nu(\gamma_2\rho)\} \times \frac{i}{\gamma_2^2} \left[\frac{i\nu\beta}{\rho} \{\Gamma K_\nu(\gamma_2\rho) + \Phi I_\nu(\gamma_2\rho)\} \right.\right.\right.$$
$$\left.\left.\left. + \omega\varepsilon_2\gamma_2 \left\{\Theta K'_\nu(\gamma_2\rho) + \Lambda I'_\nu(\gamma_2\rho)\right\} \right] - \{\Gamma K_\nu(\gamma_2\rho) + \Phi I_\nu(\gamma_2\rho)\} \right.$$
$$\times \frac{i}{\gamma_2^2} \left[\frac{i\nu\beta}{\rho} \{\Theta K_\nu(\gamma_2\rho) + \Lambda I_\nu(\gamma_2\rho)\} \right.$$
$$\left.\left. -\omega\mu_0\gamma_2 \left\{\Gamma K'_\nu(\gamma_2\rho) + \Phi I'_\nu(\gamma_2\rho)\right\} \right] \right] \rho d\rho d\phi \Big| \tag{11}$$

and

$$P_{oc} = \pi \left| \int_{\rho_b}^{\infty} \mathrm{Re} \left[\Xi K_\nu(\gamma_3\rho) \times \frac{i}{\gamma_3^2} \left\{ \frac{i\nu\beta}{\rho} \Psi K_\nu(\gamma_3\rho) + \omega\varepsilon_3\Xi\gamma_3 K'_\nu(\gamma_3\rho) \right\} \right.\right.$$
$$\left.\left. -\Psi K_\nu(\gamma_3\rho) \times \frac{i}{\gamma_3^2} \left\{ \frac{i\nu\beta}{\rho} \Theta K_\nu(\gamma_3\rho) - \omega\mu_0\Psi\gamma_3 K'_\nu(\gamma_3\rho) \right\} \rho d\rho d\phi \right| \tag{12}$$

In the above Eqs. (10), (11) and (12), ν is the mode-designating parameter that can take only discrete values and various other symbols have their meanings as follows:

$$\Phi=\frac{(c_3n_3-b_3o_3)(a_3f_3-b_3e_3-a_3j_3+b_3i_3)+(a_3n_3-b_3m_3)(c_3j_3-b_3k_3-a_3n_3+b_3m_3)}{(c_3n_3-b_3o_3)(d_3j_3-b_3l_3-d_3f_3+b_3h_3)+(d_3n_3-b_3p_3)(c_3f_3-b_3g_3-c_3j_3+b_3k_3)},$$

$$\Gamma=\frac{(b_3h_3-d_3f_3)\Phi+(b_3e_3-a_3f_3)}{(c_3f_3-b_3g_3)},\quad \Lambda=-\left(\frac{a_3+c_3\Gamma+d_3\Phi}{b_3}\right),$$

$$\Theta=-\left(\frac{x_4\Lambda+x_5\Gamma+x_6\Phi}{x_3}\right),\quad \Omega=-\frac{x_1}{x_2},$$

$$\Xi=\frac{(y_7y_{14}-y_8y_{13})\Lambda+(y_9y_{13}-y_7y_{15})\Gamma+(y_{10}y_{13}-y_7y_{16})\Phi}{y_7y_{17}-y_{11}y_{13}+\frac{y_5}{y_6}(y_7y_{18}-y_{12}y_{13})},\quad \Psi=-\frac{y_5}{y_6}\Xi,$$

$$a_3=x_3\left(x_7-\frac{x_1x_8}{x_2}\right),\quad b_3=x_4x_9-x_3x_{10},\quad c_3=x_5x_9+x_3x_{11},$$

$$d_3=x_6x_9+x_3x_{12},\quad e_3=x_3\left(x_{13}+\frac{x_1x_{14}}{x_2}\right),\quad f_3=x_4x_{15}-x_3x_{16},$$

$$g_3=x_5x_{15}+x_3x_{17},\quad h_3=x_6x_{15}+x_3x_{18},\quad i_3=y_1\left(x_7-\frac{x_1x_8}{x_2}\right),$$

$$j_3=x_9y_2-x_{10}y_1,\quad k_3=x_{11}y_1+x_9y_3,\quad l_3=x_9y_4+x_{12}y_1,$$

$$m_3=y_1\left(x_{13}+\frac{x_1x_{14}}{x_2}\right),\quad n_3=x_{15}y_2-x_{16}y_1,\quad o_3=x_{15}y_3+x_{17}y_1,$$

$$p_3=x_{15}y_4+x_{18}y_1,\quad x_1=\left(\sin\psi+\frac{\nu\beta}{\gamma_1^2\rho_a}\cos\psi\right)J_\nu(\gamma_1\rho_a),$$

$$x_2=\frac{i\omega\mu_0}{\gamma_1}\cos\psi J'_\nu(\gamma_1\rho_a),\quad x_3=\left(\sin\psi+\frac{\nu\beta}{\gamma_2^2\rho_a}\cos\psi\right)K_\nu(\gamma_2\rho_a),$$

$$x_4=\left(\sin\psi+\frac{\nu\beta}{\gamma_2^2\rho_a}\cos\psi\right)I_\nu(\gamma_2\rho_a),\quad x_5=\frac{i\omega\mu_0}{\gamma_2}\cos\psi K'_\nu(\gamma_2\rho_a);$$

$$x_6=\frac{i\omega\mu_0}{\gamma_2}\cos\psi I'_\nu(\gamma_2\rho_a),\quad x_7=\left(\cos\psi-\frac{\nu\beta}{\gamma_1^2\rho_a}\sin\psi\right)J_\nu(\gamma_1\rho_a),$$

$$x_8=\frac{i\omega\mu_0}{\gamma_1}J'_\nu(\gamma_1\rho_a),\quad x_9=\left(\cos\psi-\frac{\nu\beta}{\gamma_2^2\rho_a}\sin\psi\right)K_\nu(\gamma_2\rho_a),$$

$$x_{10}=\left(\cos\psi-\frac{\nu\beta}{\gamma_2^2\rho_a}\sin\psi\right)I_\nu(\gamma_2\rho_a),\quad x_{11}=\frac{i\omega\mu_0}{\gamma_2}\sin\psi K'_\nu(\gamma_2\rho_a),$$

$$x_{12}=\frac{i\omega\mu_0}{\gamma_2}\sin\psi I'_\nu(\gamma_2\rho_a),\quad x_{13}=\frac{i\omega\varepsilon_1}{\gamma_1}\cos\psi J'_\nu(\gamma_1\rho_a),$$

$$x_{14}=\left(\sin\psi+\frac{\nu\beta}{\gamma_1^2\rho_a}\cos\psi\right)J_\nu(\gamma_1\rho_a),\quad x_{15}=\frac{i\omega\varepsilon_2}{\gamma_2}\cos\psi K'_\nu(\gamma_2\rho_a),$$

$$x_{16}=\frac{i\omega\varepsilon_2}{\gamma_2}\cos\psi I'_\nu(\gamma_2\rho_a),\quad x_{17}=\left(\sin\psi+\frac{\nu\beta}{\gamma_2^2\rho_a}\cos\psi\right)K_\nu(\gamma_2\rho_a),$$

$$x_{18}=\left(\sin\psi+\frac{\nu\beta}{\gamma_2^2\rho_a}\cos\psi\right)I_\nu(\gamma_2\rho_a),\quad y_1=\left(\sin\psi+\frac{\nu\beta}{\gamma_2^2\rho_b}\cos\psi\right)K_\nu(\gamma_2\rho_b),$$

$$y_2=\left(\sin\psi+\frac{\nu\beta}{\gamma_2^2\rho_b}\cos\psi\right)I_\nu(\gamma_2\rho_b),\quad y_3=\frac{i\omega\mu_0}{\gamma_2}\cos\psi K'_\nu(\gamma_2\rho_b)$$

$$y_4=\frac{i\omega\mu_0}{\gamma_2}\cos\psi I'_\nu(\gamma_2\rho_b),\quad y_5=\left(\sin\psi+\frac{\nu\beta}{\gamma_3^2\rho_b}\cos\psi\right)K_\nu(\gamma_3\rho_b),$$

$$y_6=\frac{i\omega\mu_0}{\gamma_3}\cos\psi K'_\nu(\gamma_3\rho_b),\quad y_7=\left(\cos\psi-\frac{\nu\beta}{\gamma_2^2\rho_b}\sin\psi\right)K_\nu(\gamma_2\rho_b),$$

$$y_8=\left(\cos\psi-\frac{\nu\beta}{\gamma_2^2\rho_b}\sin\psi\right)I_\nu(\gamma_2\rho_b),\quad y_9=\frac{i\omega\mu_0}{\gamma_2}K'_\nu(\gamma_2\rho_b),$$

$$y_{10}=\frac{i\omega\mu_0}{\gamma_2}I'_\nu(\gamma_2\rho_b),\quad y_{11}=\left(\cos\psi-\frac{\nu\beta}{\gamma_3^2\rho_b}\sin\psi\right)K_\nu(\gamma_3\rho_b),$$

$$y_{12}=\frac{i\omega\mu_0}{\gamma_3}\sin\psi K'_\nu(\gamma_3\rho_b),\quad y_{13}=\frac{i\omega\varepsilon_2}{\gamma_2}\cos\psi K'_\nu(\gamma_2\rho_b),$$

$$y_{14}=\frac{i\omega\varepsilon_2}{\gamma_2}\cos\psi I'_\nu(\gamma_2\rho_b),\quad y_{15}=\left(\sin\psi+\frac{\nu\beta}{\gamma_2^2\rho_b}\cos\psi\right)K_\nu(\gamma_2\rho_b),$$

$$y_{16}=\left(\sin\psi+\frac{\nu\beta}{\gamma_2^2\rho_b}\cos\psi\right)I_\nu(\gamma_2\rho_b),\quad y_{17}=\frac{i\omega\varepsilon_3}{\gamma_3}\cos\psi K'_\nu(\gamma_3\rho_b),$$

and $$y_{18}=\left(\sin\psi+\frac{\nu\beta}{\gamma_3^2\rho_b}\cos\psi\right)K_\nu\left(\gamma_3\rho_b\right).$$

In Eqs. (10), (11) and (12), P_{ic}, P_c and P_{oc} are, respectively, the power propagating through the HCLCF core, the inner dielectric clad and the outermost liquid crystal clad sections. It is to be noted at this point that, for the evaluation of power, the values of all the arbitrary constants (C_{ϕ_1}, C_{ϕ_2}, C_{ϕ_3} and C_{ϕ_4}) are evaluated in terms of one constant (say C_{ϕ_1}), which can be determined by a normalization condition taking into consideration the input power. If P_t describes the total power transmitted by the transverse electric modes through the HCLCF under consideration, i.e.,

$$P_t = P_c + P_{ic} + P_{oc}, \tag{13}$$

then P_c/P_t ($\equiv \xi_c$), P_{ic}/P_t ($\equiv \xi_{ic}$), and P_{oc}/P_t ($\equiv \xi_{oc}$) will, respectively, represent the relative power distributions in the HCLCF core, the inner clad and the outermost liquid crystal regions.

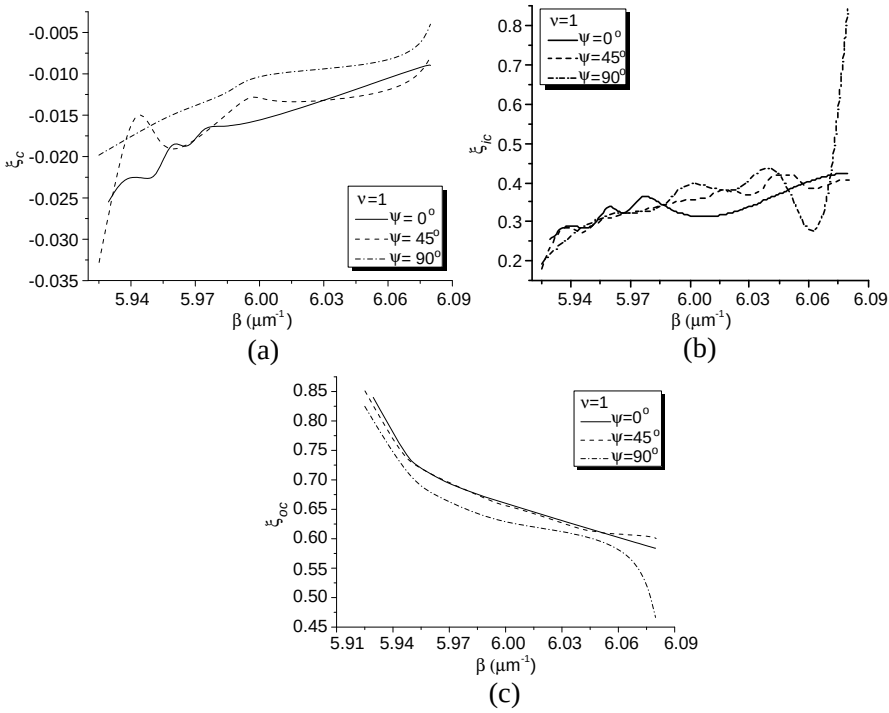

Figure 3. (a) Core confinement power versus propagation constant for different pitch angles. (b) Inner cladding confinement power versus propagation constant for different pitch angles. (c) Outer cladding confinement power versus propagation constant for different pitch angles.

3. RESULTS AND DISCUSSION

We are now in a position to analyze the effect of helical windings on the power confinement factors in the three different sections of the HCLCF. Within the context, we emphasize on the relative power distribution upon which the helix pitch angle is considered to have the controlling property. As stated earlier, for the sake of simplicity, we assume that the core/clad sections are non-magnetic in nature, which leads to the situation $\mu_1 = \mu_2 = 0$. Figures 3 and 4, respectively, show the variation of the power confinement factors (or the relative power) with the propagation constant β corresponding to the azimuthal index values as $\nu = 1$ and $\nu = 2$ under the situation of transverse electric (TE) mode excitation. The RI values of core and the inner cladding sections are considered as $n_1 = 1.462$ and $n_2 = 1.458$, respectively. In our illustrative case, for the outermost section, we used the nematic liquid

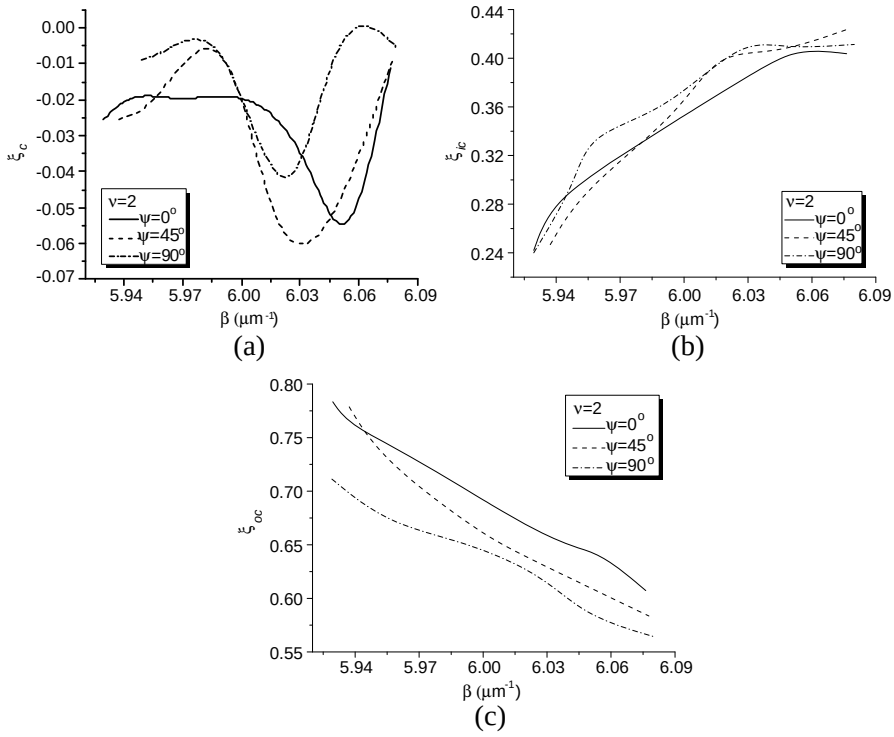

Figure 4. (a) Core confinement power versus propagation constant for different pitch angles. (b) Inner cladding confinement power versus propagation constant for different pitch angles. (c) Outer cladding confinement power versus propagation constant for different pitch angles.

crystal as BDH mixture 14616, which has ordinary and extraordinary RI values as $n_o = 1.457$ and $n_e = 1.5037$, respectively. The operating wavelength λ_0 is kept fixed as 1550 nm since most of the optical components operate at this wavelength. Also, the introduced values of the angle of pitch are taken to be 0°, 45° and 90°. We now concentrate on the illustration of the power confinement factor ξ, the variation of which is plotted against the allowed values of the propagation constant β corresponding to the different values of pitch angle ψ. Further, in our illustrative case, the core and the inner clad diameters are taken to be 90 μm and 120 μm, respectively.

Figures 3(a), 3(b) and 3(c), respectively, illustrate the variation of the power confinement factors (against the propagation constant β) in the core, inner clad and the outer clad sections of the fiber under the excitation of low order TE modes, and the helix pitch angles

as 0°, 45° and 90°. We observe from Figure 3(a) that the power confinement in the fiber core generally increases with the increase in propagation constant. Furthermore, the minimum amount of power is transported corresponding to the situation when the helix pitch angle is 0°, i.e., when the windings are perpendicular to the optical axis. Corresponding to 90° pitch angle, the power remains maximum in this region; in this case the windings are parallel to the optical axis of the guide, which virtually retains the physical properties of the structure under the usual circumstance. As such, the helical windings at the core and the inner clad boundary essentially play the role to attenuate the power in the core section of the guide. In other words, the pitch angle of the helix can be adjusted according to the operation/measurement needs.

In the inner clad region too (Figure 3(b)), the power patterns generally exhibit an increase with increasing β-values; however, the increase is much smaller as compared to what observed in the core region of the HCLCF. We find that the variation of power in this region remains primarily within the range of 20% to 50% except a blow-up near the higher tail of the allowed values of β corresponding to the situation when the windings are parallel to the optical axis of the guide. Also, the angle of helix pitch certainly has the effect on the control of power as the 0° pitch angle attenuates the power much near the higher tail of the propagation constant; 45° pitch makes to release the power a little.

Corresponding to Figure 3(c), which depicts the power pattern in the outermost liquid crystal section of the guide, we observe that the power decreases with the increase in propagation constant. Also, within the allowed values of the propagation constant, almost 50% to 85% of power exists in this section. The high amount of power confinement in this region is essentially attributed to the existence of the radial anisotropy in this section. Furthermore, not much difference is observed in the power pattern corresponding to the situations of 0° and 45° pitch angle; helical wraps parallel to optical axis certainly reduces the power a little. Thus, the noticeable fact can be drawn that the structure allows to confine the maximum amount of power in the outermost liquid crystal section of the guide, and the confinement pattern can be altered by changing the pitch angle of the helical wraps loaded on the interface of the core and the inner dielectric clad sections.

Considering the case of the next higher order modes corresponding to $\nu = 2$, we observe that, within the fiber core, the power pattern remains oscillatory (Figure 4(a)) with minimum oscillations for the case of helical windings in the perpendicular direction, i.e., $\psi = 0°$. Further, the power in this region remains extremely small with the

minimum amount of power corresponding to the situation with 0° pitch angle, which determines the power attenuation property of the helical windings. At this point, it is to be noted that the fiber parameters as well as the operating wavelength are kept unchanged, and the oscillatory behavior of the power pattern may be attributed to the more dispersion of waves happening in the case of higher order modes. From Figure 4(b) we find that the confinement increases with the increase in the values of the propagation constants, and it remains within the range of 25%–45%, which is in the almost similar range as observed in Figure 3(b) corresponding to the situation of low order modes with $\nu = 1$; the minimum power is transported during the situation when the helical wraps are perpendicular to the direction of propagation. However, the shoot-up of power is not observed in the case of higher order modes. Instead, the power is distributed in this case, which is very much expected.

In the outermost liquid crystal clad (Figure 4(c)), we observe that the trend of the power pattern is similar to that observed in the case of Figure 3(c), i.e., it decreases with the increase in the values of β. Moreover, the power is enormously increased, and it lies almost within the range of 57%–77%, which is certainly a little less than that observed in Figure 3(c) corresponding to the situation of modes with the azimuthal index $\nu = 1$. This is essentially due to the reason of considering higher modes, which generally reduces the transportation of power owing to possible dispersion inside. We further observe that the minimum amount of power is transported when the helical windings are parallel to the longitudinal axis of the fiber, which is similar to the situation noticed in the case of Figure 3(c); the fiber under perpendicular helical wraps transmits the maximum amount of power, and the wrapping with 45° pitch angle makes the guide to sustain the power to lie in between the situations of parallel and perpendicular (to the optical axis) wraps. We, thus, observe that the liquid crystal section makes the guiding structure to confine the maximum amount of power, and also, the helical windings have the feature to control the transmission of power through the guide.

It is to be noted at this point that Choudhury et al. reported earlier the investigations of multilayered cylindrical dielectric fibers [27, 28] with annular core geometry. It was reported that the confinement of power in the core section (which is sandwiched between two dielectric clads) increases for annular core fibers of larger cross-sectional dimensions. Such annular core fibers with different types of materials (e.g., chirowaveguides made of chiral materials [21, 29] having optical activity) in the core and the cladding sections have also been reported with the mention of their potentiality in the area of

optical sensors based on the study of evanescent wave spectroscopy, e.g. chemical sensing. In reality, various forms of waveguides made of chiral metamaterials have been reported in the literature, and their potentialities have been discussed [30–40].

The use of liquid crystal fibers in optical sensing has been reported before. However, by making the liquid crystal fiber loaded with helical windings is essentially a new concept which, to the best of knowledge of the author, has not yet been discussed in the literature. In the present study of twisted clad liquid crystal fibers, we observe that much amount of power is confined in the outer liquid crystal section, which can further be controlled through the proper structuring of the helical wraps. This way, the guide enhances the sensitivity, as demonstrated in the present paper through rigorous analytical treatments. Chemical sensing may be one of the areas where such fibers could be used, as these would be greatly useful in sensing even weak chemical reactions because of sustaining very high amount of power confinement in the outermost liquid crystal section. Apart from that, such structures may be effectively used as field coupling components. As to the optical sensing needs, it is presumed that the implementation of such twisted clad liquid crystal fibers for sensing would be comparatively easier as the launching of optical power would not be that difficult which one may face in the case of annular core fibers.

4. CONCLUSION

From the foregoing discussion, it can be inferred that HCLCFs can support a very high amount of power in the outermost region of the guide — the phenomenon that would find prominent applications in the area of integrated optics and/or optical sensing. The presence of helical windings at the core-inner clad boundary allows to control the flow of power through the guide by suitably adjusting the angle of pitch, which is effective in the outermost liquid crystal section as well. It has been observed that the excitation of higher order modes reduces the transportation of power, which is as usually observed in the study of the propagation characteristics of optical fibers.

ACKNOWLEDGMENT

This work is supported by the Fundamental Research Grant Project (FRGS/1/2011/TK/UKM/01/16) by the Ministry of Higher Education (Malaysia); the author is thankful to the Ministry. Also, he is grateful to the anonymous reviewer to make some general comments on the paper, according to which the author could modify the text partially with a better presentation.

REFERENCES

1. Wu, S.-T. and U. Efron, "Optical properties of thin nematic liquid crystal cells," *Appl. Phys. Lett.*, Vol. 48, 624–636, 1986.
2. Winter, C. S., J. D. Rush, and D. G. Smith, "Liquid crystal materials' refractive index matched to silica," *Liq. Cryst.*, Vol. 2, 561–564, 1987.
3. Sage, I. and D. Chaplin, "Low RI liquid crystals for integrated optics," *Electron. Lett.*, Vol. 23, 1192–1193, 1987.
4. Green, M. and S. J. Madden, "Low loss nematic liquid crystal cored fiber waveguides," *Appl. Opt.*, Vol. 28, 5202–5203, 1989.
5. Lin, H., P. P. Muhoray, and M. A. Lee, "Liquid crystalline cores for optical fibers," *Mol. Cryst. Liq. Cryst.*, Vol. 204, 189–200, 1991.
6. Goldburt, E. S. and P. S. J. Russell, "Electro-optical response of a liquid-crystalline fiber coupler," *Appl. Phys. Lett.*, Vol. 48, 10–12, 1986.
7. Veilleux, C., J. Lapierre, and J. Bures, "Liquid-crystal-clad tapered fibers," *Opt. Lett.*, Vol. 11, 733–735, 1986.
8. Chen, S.-H. and T. J. Chen, "Observation of mode selection in a radially anisotropic cylindrical waveguide with liquid-crystal cladding," *Appl. Phys. Lett.*, Vol. 64, 1893–1895, 1994.
9. Busurin, V. I., M. Green, J. R. Cozens, and K. D. Leaver, "Switchable coaxial optical coupler using a liquid crystal mixture," *Appl. Phys. Lett.*, Vol. 42, 322–324, 1983.
10. Liu, K., W. V. Sorin, and H. J. Shaw, "Single-mode-fiber evanescent polarizer/amplitude modulator using liquid crystals," *Opt. Lett.*, Vol. 11, 180–182, 1986.
11. El-Sherif, M. A., P. M. Shankar, P. R. Herczfeld, L. Bobb, and H. Krumboltz, "On-fiber electrooptic modulator/switch," *Appl. Opt.*, Vol. 25, 2469–2470, 1986.
12. Kashyap, R., C. S. Winter, and B. K. Nayar, "Polarization desensitized liquid-crystal overlay optical-fiber modulator," *Opt. Lett.*, Vol. 13, 401–403, 1988.
13. Ioannidis, Z. K., I. P. Giles, and C. Bowry, "All-fiber optic intensity modulators using liquid crystals," *Appl. Opt.*, Vol. 30, 328–333, 1991.
14. Yoshino, T., Y. Takahashi, H. Tamura, and N. Ohde, "Some special fibers for distributed sensing of uv light, electric field or strain," *Proc. SPIE*, Vol. 2071, 242–254, 1993.
15. Pierce, J. R., *Travelling Wave Tubes*, D. Van Nostrand, NJ, 1950.
16. Kumar, D. and O. N. Singh, II, "Modal characteristic equation

and dispersion curves for an elliptical step-index fiber with a conducting helical winding on the core-cladding boundary — An analytical study," *J. Light. Tech.*, Vol. 20, 1416–1424, 2002.

17. Kumar, D., P. K. Choudhury, and F. A. Rahman, "Towards the characteristic dispersion relation for step-index hyperbolic waveguide with conducting helical winding," *Progress In Electromagnetics Research*, Vol. 71, 251–275, 2007.
18. Kumar, D., P. K. Choudhury, and O. N. Singh, II, "Towards the dispersion relations for dielectric optical fibers with helical windings under slow- and fast-wave considerations — A comparative analysis," *Progress In Electromagnetics Research*, Vol. 80, 409–420, 2008.
19. Siong, C. C. and P. K. Choudhury, "Propagation characteristics of tapered core helical clad dielectric optical fibers," *Journal of Electromagnetic Waves and Applications*, Vol. 23, No. 5, 663–674, 2009.
20. Safie, A. H. B. M. and P. K. Choudhury, "On the field patterns of helical clad dielectric optical fibers," *Progress In Electromagnetics Research*, Vol. 91, 69–84, 2009.
21. Lim, K. Y., P. K. Choudhury, and Z. Yusoff, "Chirofibers with helical windings — An analytical investigation," *Optik*, Vol. 121, 980–987, 2010.
22. Choudhury, P. K. and D. Kumar, "On the slow-wave helical clad elliptical fibers," *Journal of Electromagnetic Waves and Applications*, Vol. 24, Nos. 14–15, 1931–1942, 2010.
23. Snyder, A. W. and F. Rühl, "Single-mode, single-polarization fibers made of birefringent material," *J. Opt. Soc. Am.*, Vol. 73 1165–1174, 1983.
24. Chen, Y., "Anisotropic fiber with cylindrical polar axes," *Appl. Phys. B*, Vol. 42, 1–3, 1987.
25. Watkins, D. A., *Topics in Electromagnetic Theory*, Wiley, USA, 1958.
26. Cherin, A. H., *An Introduction to Optical Fibers*, Chapter 5, McGraw-Hill, New York, 1987.
27. Choudhury, P. K. and R. A. Lessard, "An estimation of power transmission through a doubly clad optical fiber with annular core," *Microw. and Opt. Technol. Lett.*, Vol. 29, 402–405, 2001.
28. Choudhury, P. K. and T. Yoshino, "A rigorous analysis of the power distribution in plastic clad annular core optical fibers," *Optik,* Vol. 113, 481–488, 2002.
29. Nair, A. and P. K. Choudhury, "On the analysis of field patterns in

chirofibers," *Journal of Electromagnetic Waves and Applications*, Vol. 21, No. 15, 2277–2286, 2007.

30. Tuz, V. R. and C.-W. Qiu, "Semi-infinite chiral nihility photonics: Parametric dependence, wave tunneling and rejection," *Progress In Electromagnetics Research*, Vol. 103, 139–152, 2010.
31. Ahmed, S. and Q. A. Naqvi, "Electromagnetic scattering from a chiral-coated nihility cylinder," *Progress In Electromagnetics Research Letters*, Vol. 18, 41–50, 2010.
32. Naqvi, A., S. Ahmed, and Q. A. Naqvi, "Perfect electromagnetic conductor and fractional dual interface placed in a chiral nihility medium," *Journal of Electromagnetic Waves and Applications*, Vol. 24, Nos. 14–15, 1991–1999, 2010.
33. Naqvi, A., A. Hussain, and Q. A. Naqvi, "Waves in fractional dual planar waveguides containing chiral nihility metamaterial," *Journal of Electromagnetic Waves and Applications*, Vol. 24, Nos. 11–12, 1575–1586, 2010.
34. Wu, Z., B. Q. Zeng, and S. Zhong, "A double-layer chiral metamaterial with negative index," *Journal of Electromagnetic Waves and Applications*, Vol. 24, No. 7, 983–992, 2010.
35. Topa, A. L., C. R. Paiva, and A. M. Barbosa, "Electromagnetic wave propagation in chiral H-guides," *Progress In Electromagnetics Research*, Vol. 103, 285–303, 2010.
36. Canto, J. R., C. R. Paiva, and A. M. Barbosa, "Dispersion and losses in surface waveguides containing double negative or chiral metamaterials," *Progress In Electromagnetics Research*, Vol. 116, 409–423, 2011.
37. Li, J., F.-Q. Yang, and J. Dong, "Design and simulation of L-shaped chiral negative refractive index structure," *Progress In Electromagnetics Research*, Vol. 116, 395–408, 2011.
38. Dong, J., J. Li, and F.-Q. Yang, "Guided modes in the four-layer slab waveguide containing chiral nihility core," *Progress In Electromagnetics Research*, Vol. 112, 241–255, 2011.
39. Baqir, M. A., A. A. Syed, and Q. A. Naqvi, "Electromagnetic fields in a circular waveguide of chiral nihility metamaterial," *Progress In Electromagnetics Research M*, Vol. 16, 85–93, 2011.
40. Dong, J. and J. Li, "Characteristics of guided modes in uniaxial chiral circular waveguide," *Progress In Electromagnetics Research*, Vol. 124, 331–345, 2012.